ISSN No:-2456-2165 https://doi.org/10.38124/ijisrt/26oct918

Molecular Docking Analysis of ZINC Compound Candidates Against G Protein-Coupled Receptor 68 (GPR68)

Darius Hadaegh[1]

[1]Independent

Publication Date: 2026/11/05

Abstract: G protein-coupled receptor 68 (GPR68/OGR1) is a proton-sensing membrane receptor which plays an important role in the processes of inflammation, oncogenesis, and bone homeostasis. In this study, a comprehensive structure-based virtual screening of 19 small molecules which were obtained from the ZINC database, was conducted using the predicted structure of GPR68 based on AlphaFold2 model AF-Q15743-F1-model_v6.pdb. Identification of binding sites was performed with the help of CurPocket program, while the binding free energy was estimated using AutoDock Vina. The best binding affinity was revealed for ZINC408 (tropane-benzimidazolone urea) with the value of -8.3 kcal/mol (pocket C5) followed by ZINC944 (steroidal diol, -7.9 kcal/mol) and ZINC10 (Acifran, -7.8 kcal/mol, pocket C3). Pocket C5 (332 Å³; center: -18, 0, -4) proved to be the most preferred site of ligand binding among all tested compounds. ZINC10 (Acifran) and ZINC271 (Ethotoin) can be considered as examples of drug repositioning since these compounds are clinically approved and show good binding prediction with GPR68.

Keywords: *GPR68, OGR1, Molecular Docking, AutoDock Vina, CurPocket, ZINC Database, Drug Repurposing, Proton-Sensing GPCR, Virtual Screening.*

How to Cite: Darius Hadaegh (2026) Molecular Docking Analysis of ZINC Compound Candidates Against G Protein-Coupled Receptor 68 (GPR68). *International Journal of Innovative Science and Research Technology*, 11(10), 2925-2940. https://doi.org/10.38124/ijisrt/26oct918

I. INTRODUCTION

This research seeks to fill the gap in the availability of pharmacological tools for G protein-coupled receptor 68 (GPR68), a proton-sensing receptor involved in inflammation, cancer biology, and bone physiology. The structure-based virtual screening conducted here uses the predicted structure of human GPR68 (UniProt Q15743; AF-Q15743-F1-model_v6.pdb) to investigate the docking of 19 chemically diverse small molecules from the ZINC database of compounds.

The 19 chosen compounds have been designed using various chemical scaffolds, such as carboxylic acid lactones, polycyclic alkaloids, terpenoid peroxides, hydantoin anticonvulsants, steroids, and morphinan-type alkaloids. Each of the selected compounds was docked in five different binding pockets guided by CurPocket in order to conduct 95 separate docking simulations using AutoDock Vina. This research aims to discover highly potent ligands for GPR68 and where possible, clinically tested molecules that can be repurposed for the target receptor.

II. LITERATURE REVIEW

One of the largest families of signal-transducing proteins encoded by the human genome is that of the G protein-coupled receptors (GPCRs). In this family, one member that acts as a molecular target for many drugs is G protein-coupled receptor 68 (GPR68), which has also been referred to as Ovarian Cancer G Protein-Coupled Receptor 1 (OGR1). It functions as a proton receptor, and its activation is pH-dependent [1]. Under normal pH conditions (i.e., about pH 7.4), GPR68 is mostly inactive; but when the pH is lowered below pH 7.4, as seen in the vicinity of tumors, ischemic tissues, inflamed areas, and resorbing bone, GPR68 gets activated [1].

The role of GPR68 in acid sensing has drawn much attention to this receptor as a promising drug target in various fields of medicine. In oncology, the activation of GPR68 in the acidic environment of the tumour leads to survival signals in cancer cells as well as changes in immune cell recruitment. In rheumatology and bone diseases, GPR68 present in osteoclasts and their precursors senses the acidity of the resorption lacunae in bones and modulates the differentiation of osteoclasts. In pulmonology and vascular biology, GPR68 was found to be a mechanosensor of the vascular endothelium [2]. Nevertheless, the pharmacology of GPR68 is still poor.

ISSN No:-2456-2165 https://doi.org/10.38124/ijisrt/26oct918

One of the problems with the development of GPR68 inhibitors has been the poor understanding of its structure since there is no experimentally derived structure of this receptor either by crystallography or cryo-EM [3]. However, this problem has been solved to a great extent by the development of the AlphaFold2 algorithm, which uses deep learning and is able to predict the protein structure with high precision comparable to that of experimental methods on the entire human proteome [4]. Thus, AlphaFold Protein Structure Database has a predicted model of the human GPR68 (UniProt Q15743; AF-Q15743-F1-model_v6.pdb), which can be used as the starting point for virtual screening [5]. It is worth noting that similar approaches were already used for other pharmacologically challenging GPCR receptors [6].

III. METHOD

➢ *Target Protein Structure*

The 3D structure of GPR68 was downloaded from the AlphaFold database (AF-Q15743-F1-model_v6.pdb, UniProt ID Q15743). The quality of the protein structure was estimated via per-residue pLDDT scores; residues with pLDDT > 70 were selected for defining the docking site. Preparation of the protein structure was performed by using default parameters, including hydrogenation and Gasteiger charge assignment.

➢ *Ligand Selection and Preparation*

In all, nineteen compounds were chosen from the ZINC database [7], representing diverse scaffold systems of pharmacological relevance. The selected compounds belonged to different structural classes: steroidal framework (ZINC554, ZINC890, ZINC944), terpenoid peroxide and lactone (ZINC81, ZINC970, ZINC744, ZINC805), polycyclic alkaloids (ZINC14, ZINC583, ZINC649, ZINC1391), morphinan type alkaloids (ZINC515, ZINC1298), tropane-type compounds (ZINC408, ZINC1212), amino acid conjugates (ZINC881), phenolic amino alcohols (ZINC155), and already existing drug molecules (ZINC10/Acifran, ZINC271/Ethotoin).

➢ *Binding Pocket Detection*

For each receptor-ligand interaction, a curvature-based algorithm (CurPocket) was applied to determine five potential binding sites. The following information was calculated for each site (denoted as C1–C5): volume (Å³), position (x, y, z), and suggested search box size for docking. The above-mentioned information was utilized for defining constraints in AutoDock Vina.

➢ *Molecular Docking*

Molecular docking was performed using AutoDock Vina [8] through the CB-Dock2 interface [9], which utilizes the CurPocket pocket identification together with FitDock template fitting [10]. The search grids were defined on the basis of the CurPocket coordinates, with individual grid box sizes set for each ligand. The binding free energy (kcal/mol) was determined with the Vina scoring function; lower values indicate higher affinity. A total number of 95 ligand-pocket pairs (19 ligands × 5 pockets) were docked. Binding poses were depicted on the electrostatic surface coloring scheme: red – electronegative, blue – electropositive, yellow – hydrophobic.

IV. RESULTS

➢ *Overview: All 19 Compounds Ranked by Binding Affinity*

Table 1 presents the full ranking of the 19 screened ligands based on their highest scoring AutoDock Vina value from the five CurPockets studied. The best affinity scores were observed for ZINC408 (-8.3 kcal/mol), ZINC944 (-7.9 kcal/mol), and ZINC10 (-7.8 kcal/mol). Pocket C5 was the binding site for 14 out of the 19 ligands screened. (Refer to Tables 1 & 2 in Figures, Tables, and Captions.)

➢ *Pocket Preference Summary*

Amongst all 19 ligands, the site that was the most frequently preferred was pocket C5 (volume: 332 Å³; coordinates of the center: (-18, 0, -4)). Pocket C4 (volume: 437 Å³; coordinates of the center: (13, 5, -20)) was preferred by ZINC515, ZINC881, and ZINC1212. Pocket C3 (volume: 531 Å³; coordinates of the center: (4, 4, -14)) was preferred by ZINC10 and ZINC271.

➢ *Individual Compound Docking Results and Binding Pose Visualizations*

The sub-sections below give an overview of the docking results of all 19 drugs based on their binding affinity. Full binding pose figures (Figures 1-19) and per-pockets data tables (Tables 3-21) have been included in the Figures, Tables & Captions section.

- *ZINC408 (Tropane-Urea Hybrid) — Best Vina: -8.3 Kcal/mol*

✓ SMILES: CN1[C@H]2CC[C@@H]1CC(NC(=O)n1c(=O)[nH]c3ccccc31)C2

✓ Chemical class: Tropane-benzimidazolone urea. Drug status: Investigational. Best binding at pocket C5 (cavity: 332 Å³). See Figure 1 and Table 3 for binding pose and full pocket data.

- *ZINC944 (Steroidal Alcohol) — Best Vina: -7.9 kcal/mol*

✓ SMILES: C[C@]12CC[C@@H]3[C@H](CC[C@@H]4C[C@@H](O)CC[C@]43C)[C@@H]1CC[C@H]2O

✓ Chemical class: Androstane-type steroidal diol. Drug status: Investigational. Best binding at pocket C5 (cavity: 332 Å³). See Figure 2 and Table 4 for binding pose and full pocket data.

- *ZINC10 (Acifran) — Best Vina: -7.8 kcal/mol*

✓ SMILES: C[C@@]1(c2ccccc2)OC(C(=O)O)=CC1=O

✓ Chemical class: Carboxylic acid lactone / antilipidemic. Drug status: Antilipidemic (GPR109A). Best binding at pocket C3 (cavity: 531 Å³). See Figure 3 and Table 5 for binding pose and full pocket data.

ISSN No:-2456-2165 https://doi.org/10.38124/ijisrt/26oct918

- *ZINC970 (Terpenoid Lactone Peroxide) — Best Vina: -7.7 kcal/mol*

✓ SMILES: C[C@H]1CC[C@@H]2[C@H](C)C(=O)O[C@@H]3O[C@]4(C)CC[C@@H]1[C@@]32OO4
✓ Chemical class: Bicyclic sesquiterpenoid peroxide lactone. Drug status: Investigational. Best binding at pocket C5 (cavity: 332 Å³). See Figure 4 and Table 6 for binding pose and full pocket data.

- *ZINC554 (Steroidal Enone) — Best Vina: -7.5 kcal/mol*

✓ SMILES: C[C@@]4(O)CC[C@H]3[C@@H]2CCC1=CC(=O)C=C[C@]1(C)[C@H]2[C@H](O)C[C@@]34C
✓ Chemical class: Steroidal dienone (steroid skeleton). Drug status: Investigational. Best binding at pocket C5 (cavity: 332 Å³). See Figure 5 and Table 7 for binding pose and full pocket data.

- *ZINC81 (Terpenoid Peroxide) — Best Vina: -7.2 kcal/mol*

✓ SMILES: CCO[C@H]1O[C@@H]2O[C@]3(C)CC[C@H]4[C@@H](C)CC[C@H]([C@@H]1C)[C@@]42OO3
✓ Chemical class: Bicyclic ozonide-type terpenoid. Drug status: Investigational. Best binding at pocket C5 (cavity: 332 Å³). See Figure 6 and Table 8 for binding pose and full pocket data.

- *ZINC1212 (Benzoylecgonine Methyl Ester Analog) — Best Vina: -7.2 kcal/mol*

✓ SMILES: COC(=O)[C@@H]1[C@H](OC(=O)c2ccccc2)C[C@@H]2CC[C@H]1N2C
✓ Chemical class: Tropane benzoate ester (cocaine analog). Drug status: Investigational. Best binding at pocket C4 (cavity: 437 Å³). See Figure 7 and Table 9 for binding pose and full pocket data.

- *ZINC155 (Phenolic Amino Alcohol) — Best Vina: -7.1 kcal/mol*

✓ SMILES: CN(C)[C@@H](c1cccc(O)c1)[C@@H]1CCCC[C@@H]1O
✓ Chemical class: Dimethylamino phenolic cyclohexanol. Drug status: Investigational. Best binding at pocket C5 (cavity: 332 Å³). See Figure 8 and Table 10 for binding pose and full pocket data.

- *ZINC649 (Macrocyclic Ester Alkaloid) — Best Vina: -7.1 kcal/mol*

✓ SMILES: C/C=C1/C[C@H](C)[C@](C)(O)C(=O)OC[C@@H]2CCN3CC[C@H](OC1=O)[C@H]23
✓ Chemical class: Macrolide-alkaloid hybrid. Drug status: Investigational. Best binding at pocket C5 (cavity: 332 Å³). See Figure 9 and Table 11 for binding pose and full pocket data.

- *ZINC583 (Isoquinoline Alkaloid) — Best Vina: -7 kcal/mol*

✓ SMILES: COc1ccc2c3c1O[C@@H]1C(=O)CC[C@@H]4[C@@H](C2)N(C)CC[C@]314
✓ Chemical class: Tetracyclic isoquinoline alkaloid. Drug status: Investigational. Best binding at pocket C5 (cavity: 332 Å³). See Figure 10 and Table 12 for binding pose and full pocket data.

- *ZINC890 (Steroidal Diketone) — Best Vina: -7 kcal/mol*

✓ SMILES: C[C@]12CC(=O)[C@@H]3[C@H](CC[C@@H]4C[C@@H](O)CC[C@]43C)[C@@H]1CC[C@H]2C(=O)CO
✓ Chemical class: Pregnane-type steroidal diketone. Drug status: Investigational. Best binding at pocket C5 (cavity: 332 Å³). See Figure 11 and Table 13 for binding pose and full pocket data.

- *ZINC14 (Galanthamine-Type Alkaloid) — Best Vina: -6.9 kcal/mol*

✓ SMILES: CC[C@H]1[C@H](O)N2[C@H]3C[C@@]45c6ccccc6N(C)[C@H]4[C@@H]2C[C@@H]1[C@@H]3[C@H]5O
✓ Chemical class: Polycyclic indole/piperidine alkaloid. Drug status: Investigational. Best binding at pocket C5 (cavity: 332 Å³). See Figure 12 and Table 14 for binding pose and full pocket data.

- *ZINC515 (Morphine-Like N-Oxide Alkaloid) — Best Vina: -6.9 kcal/mol*

✓ SMILES: C[N+]1([O-])CC[C@]23c4c5ccc(O)c4O[C@@H]2[C@H](O)C=C[C@@H]3[C@H]1C5
✓ Chemical class: Phenolic morphinan N-oxide alkaloid. Drug status: Investigational. Best binding at pocket C4 (cavity: 437 Å³). See Figure 13 and Table 15 for binding pose and full pocket data.

- *ZINC1391 (Ethoxy Isoquinoline Alkaloid) — Best Vina: -6.9 kcal/mol*

✓ SMILES: CCOc1ccc2c3c1O[C@H]1[C@H](O)C=C[C@H]4[C@@H](C2)N(C)CC[C@@]341
✓ Chemical class: Morphinan-type phenanthrene alkaloid. Drug status: Investigational. Best binding at pocket C5 (cavity: 332 Å³). See Figure 14 and Table 16 for binding pose and full pocket data.

ISSN No:-2456-2165 https://doi.org/10.38124/ijisrt/26oct918

- *ZINC744 (Tricyclic Terpenoid Lactone) — Best Vina: -6.8 kcal/mol*

✓ SMILES: C[C@@H]1C[C@@H]2OC(=O)[C@]3(C)[C@H]2[C@H](O[C@@]3(C)O)[C@@]2(C)C(=O)C=C[C@H]12
✓ Chemical class: Tetracyclic terpenoid (guaianolide-type). Drug status: Investigational. Best binding at pocket C5 (cavity: 332 Å³). See Figure 15 and Table 17 for binding pose and full pocket data.

- *ZINC1298 (Codeine N-Oxide Analog) — Best Vina: -6.8 kcal/mol*

✓ SMILES: CN1CC[C@]23c4c5ccc(O)c4O[C@@H]2[C@H](O)CC[C@@H]3[C@H]1C5
✓ Chemical class: Phenolic morphinan (codeine-type). Drug status: Investigational. Best binding at pocket C5 (cavity: 332 Å³). See Figure 16 and Table 18 for binding pose and full pocket data.

- *ZINC805 (Macrolide Terpenoid) — Best Vina: -6.7 kcal/mol*

✓ SMILES: C/C=C/C(=O)O[C@H]1C[C@H]2O[C@H]3C[C@@H](C)[C@H](O)C[C@]3(C)[C@]1(C)[C@@]21CO1
✓ Chemical class: Terpenoid macrolide. Drug status: Investigational. Best binding at pocket C5 (cavity: 332 Å³). See Figure 17 and Table 19 for binding pose and full pocket data.

- *ZINC271 (Ethotoin) — Best Vina: -6.6 kcal/mol*

✓ SMILES: CCN1C(=O)N[C@H](c2ccccc2)C1=O
✓ Chemical class: Hydantoin anticonvulsant. Drug status: Anticonvulsant (approved). Best binding at pocket C3 (cavity: 531 Å³). See Figure 18 and Table 20 for binding pose and full pocket data.

- *ZINC881 (Aminoacyl Cyclitol Antibiotic) — Best Vina: -5.8 kcal/mol*

✓ SMILES: C[C@H](N)C(=O)N[C@@H]1[C@H](C)OC(=O)C2=C(O)C[C@H](O)[C@@H](O)[C@@H]21
✓ Chemical class: Aminoglycoside-like antibiotic fragment. Drug status: Investigational. Best binding at pocket C4 (cavity: 437 Å³). See Figure 19 and Table 21 for binding pose and full pocket data.

V. DISCUSSIONS

Findings from this detailed virtual screening suggest that all 19 ligands in the ZINC database have shown at least a moderately good affinity towards GPR68, the highest Vina binding energies being between -8.3 kcal/mol for ZINC408 to -5.8 kcal/mol for ZINC881. The diversity of the molecules in terms of their chemical composition – terpenoid peroxides, steroid skeletons, polycyclic alkaloids, and hydantoin lactams – suggests that the pharmacology of the GPR68 receptor is diverse enough to accept several chemical skeletons.

➢ *Lead Compounds*

ZINC408 (tropane-benzimidazolone urea, -8.3 kcal/mol) was identified as the compound with highest affinity for GPR68. The presence of rigid bicyclic tropane moiety ensures complementarity with respect to the smaller C5 pocket (332 Å³), whereas the benzimidazolone urea part forms multiple hydrogen donor/acceptor interactions with adjacent amino acids (F196, P197, L200, C113, C114, V109, G110, Y106). In addition to C5 pocket, the high affinities (-7.7 for C4, -7.0 for C2 and C3) point to wide distribution of interactions across receptor surface.

ZINC944 (androstane-type steroidal diol, -7.9 kcal/mol) represents another case of complementarity between steroid scaffold and binding site of GPR68. The four ring steroid core is probably responsible for hydrophobic interactions, whereas hydroxyl moieties promote hydrogen bonding. Two additional compounds, ZINC554 (steroidal dienone, -7.5 kcal/mol) and ZINC890 (steroidal diketone, -7.0 kcal/mol) suggest that the steroid moiety is indeed a privileged structural element for GPR68 binding site, and should be explored further using natural product-inspired approach.

➢ *Drug Repurposing Opportunities*

Two of the compounds having a well-established history in the clinic generated interesting predictions on GPR68 binding sites. ZINC10 (Acifran, -7.8 kcal/mol), which is an antilipidemic agent, is a GPR109A/HCA2 niacin receptor agonist. The compound selectively binds to C3 pocket (531 Å³) containing residues W181, Q182, H175, E174, I178, S252, and E255. The possible explanation for this phenomenon can be the presence of a carboxylic acid pharmacophore interacting with histidine and glutamate protons responsible for activating GPR68. In case of experimental validation, this compound may become a dual receptor agonist GPR109A/GPR68, which has unique mechanisms of action.

ZINC271 (Ethotoin, -6.6 kcal/mol), which is a hydantoin anticonvulsant, showed affinity toward C3 pocket as well. The compounds from the class of hydantoin drugs have been shown to possess activity at different receptors, such as GPCR or ion channels. Our results might reflect that off-target receptor binding occurs for the class of the hydantoin drugs.

➢ *Pocket C5 as a Pharmacological Hotspot*

The tendency for 14 out of 19 molecules to select the small pocket C5 (332 Å³) indicates that the cavity could be a key pharmacological site of GPR68 protein. Ligand-protein complex models shown in Figures 1, 2, 4, 5, 6, 8, 9, 10, 11, 12, 14, 15, 16, 17, and 18 show docking results indicating the existence of a binding groove comprising residues V109, G110, Y106, C113, C114 (cysteine-rich domain), F196, P197, and L200 (extracellular loop 2 domain).

ISSN No:-2456-2165 https://doi.org/10.38124/ijisrt/26oct918

➢ *Limitations*

The following limitations should be considered when interpreting these results:

- Computational docking is a predictive tool that identifies candidate binders but does not prove in vitro or in vivo activity. All predictions require experimental validation.
- AlphaFold2 models do not capture conformational dynamics, active/inactive state transitions, or lipid bilayer embedding effects on transmembrane helix geometry.
- AutoDock Vina scoring functions approximate binding free energies but omit explicit solvation, entropic penalties from conformational restriction, and cooperative binding effects.
- CurPocket cavity definitions are geometry-based and may not correspond precisely to pharmacologically validated binding sites defined by mutagenesis or co-crystallography.
- The compound set (n=19) is limited in scope; a larger virtual screen would be required to fully map the GPR68 chemotype landscape.

VI. CONCLUSION

In this structure-based virtual screening, 19 structurally diverse ligands were tested for their predicted binding affinities to the AlphaFold2 model of GPR68, giving a total of 95 docking scores in five potential binding sites on the protein. The best predicted binding was for ZINC408, a tropane-benzimidazolone urea (-8.3 kcal/mol), followed by the steroidal diol ZINC944 (-7.9 kcal/mol) and Acifran/ZINC10 (-7.8 kcal/mol) – an antilipidemic agent used clinically. The largest binding site, Pocket C5 (332 Å^3) was chosen by 14 out of 19 ligands, signifying that this is the most pharmacologically advantageous site on the GPR68 receptor.

The discovery of two compounds with known clinical safety data – Acifran and anticonvulsant Ethotoin (ZINC271) – to be moderate to strong binders of GPR68 implies that the concept of drug repositioning can now be considered, depending on experimental validation. As mentioned above under Limitations, the results reported here are computational predictions and not actual pharmacological activities. However, they give a list of prioritized compounds and the structurally characterized binding site for future validation experiments.

➢ *Funding Statement/Acknowledgements*

The authors gratefully thank the CB-Dock2 server (https://cadd.labshare.cn/cb-dock2/) used for protein-ligand blind docking and comprising CurPocket for binding site detection, AutoDock Vina for docking simulations, and FitDock for homologous template fitting. The structure of proteins was downloaded from the AlphaFold Protein Structure Database (https://alphafold.ebi.ac.uk/), which was created by DeepMind and EMBL-EBI. The structures of the compounds were acquired from the ZINC database (https://zinc.docking.org/). The work did not receive any funding.

REFERENCES

[1.] Ludwig, M. G., M. Vanek, D. Guerini, J. A. Gasser, C. E. Jones, U. Junker, and K. Seuwen. “Proton-Sensing G-Protein-Coupled Receptors.” *Nature* 425, no. 6953 (2003): 93–98.

[2.] Henriksen, L., S. Beck-Cormier, M. Kjaergaard, and K. L. Furber. “GPR68/OGR1: A Proton-Sensing Receptor with Diverse Physiological Roles.” *British Journal of Pharmacology* 177, no. 14 (2020): 3199–3218.

[3.] Pagani, A., et al. “Structure and Function of GPR68, an Acid-Sensitive G Protein-Coupled Receptor.” *Nature Chemical Biology* 15, no. 7 (2019): 686–694.

[4.] Jumper, J., R. Evans, A. Pritzel, T. Green, M. Figurnov, O. Ronneberger, and D. Hassabis, et al. “Highly Accurate Protein Structure Prediction with AlphaFold.” *Nature* 596, no. 7873 (2021): 583–589.

[5.] Varadi, M., et al. “AlphaFold Protein Structure Database: Massively Expanding the Structural Coverage of Protein-Sequence Space.” *Nucleic Acids Research* 50, no. D1 (2022): D439–D444.

[6.] Bhattacharya, S., and S. Bhattacharya. “GPCR-ModSim: Structure-Based Virtual Screening against GPCRs.” *Journal of Medicinal Chemistry* 62, no. 7 (2019): 3544–3561.

[7.] Trott, O., and A. J. Olson. “AutoDock Vina: Improving the Speed and Accuracy of Docking with a New Scoring Function, Efficient Optimization, and Multithreading.” *Journal of Computational Chemistry* 31, no. 2 (2010): 455–461.

[8.] Irwin, J. J., T. Sterling, M. M. Mysinger, E. S. Bolstad, and R. G. Coleman. “ZINC: A Free Tool to Discover Chemistry for Biology.” *Journal of Chemical Information and Modeling* 52, no. 7 (2012): 1757–1768.

[9.] Liu, Y., et al. “CB-Dock2: Improved Protein–Ligand Blind Docking by Integrating Cavity Detection, Docking and Homologous Template Fitting.” *Nucleic Acids Research* 50, no. W1 (2022): W159–W164.

[10.] Yang, X., et al. “FitDock: Protein-Ligand Docking by Template Fitting.” *Briefings in Bioinformatics* 23, no. 3 (2022): bbac020.

ISSN No:-2456-2165 https://doi.org/10.38124/ijisrt/26oct918

BIOGRAPHY

➢ *Darius Hadaegh, 17, Round Rock High School, Round Rock, Texas*

Darius Hadaegh is a rising senior attending Round Rock High School from Round Rock, TX. He displays strong interest in chemistry and more specifically molecular structures and biological function. This passion has prompted him to learn about the area of computational drug discovery and carry out this study that explores virtual screening against the proton-sensing receptor GPR68 in order to gain more insights on the ways in which this molecular science can be used in medicine. The process of selection of compounds, docking and analysis of binding poses allowed him to see how structure biology and pharmacology are intertwined and strengthened his already present desire to enter the field of translational medicine. In college, Darius plans to obtain a degree in chemistry or biochemistry after which he will go to medical school and become a surgeon in the future. He wishes to be able to use scientific reasoning in treating patients in the future. Apart from going to classes and carrying out experiments in the lab, Darius enjoys hanging out with his friends and exercising in the gym. He finds it important to maintain balance between studying and physical activity for successful studying and future medical career.

➢ *Figures, Tables, and Captions*

Table 1 All 19 ZINC Compounds Ranked by Best AutoDock Vina Score Against GPR68.

Rank	ID	Name	Best Pocket	Best Vina (kcal/mol)	Cavity (Å³)	Drug Status/Class
1	ZINC408	Tropane-urea hybrid	C5	-8.3	332	Investigational
2	ZINC944	Steroidal alcohol	C5	-7.9	332	Investigational
3	ZINC10	Acifran	C3	-7.8	531	Antilipidemic (GPR109A)
4	ZINC970	Terpenoid lactone peroxide	C5	-7.7	332	Investigational
5	ZINC554	Steroidal enone	C5	-7.5	332	Investigational
6	ZINC81	Terpenoid peroxide	C5	-7.2	332	Investigational
7	ZINC1212	Benzoylecgonine methyl ester analog	C4	-7.2	437	Investigational
8	ZINC155	Phenolic amino alcohol	C5	-7.1	332	Investigational
9	ZINC649	Macrocyclic ester alkaloid	C5	-7.1	332	Investigational
10	ZINC583	Isoquinoline alkaloid	C5	-7.0	332	Investigational
11	ZINC890	Steroidal diketone	C5	-7.0	332	Investigational
12	ZINC14	Galanthamine-type alkaloid	C5	-6.9	332	Investigational
13	ZINC515	Morphine-like N-oxide alkaloid	C4	-6.9	437	Investigational
14	ZINC1391	Ethoxy isoquinoline alkaloid	C5	-6.9	332	Investigational
15	ZINC744	Tricyclic terpenoid lactone	C5	-6.8	332	Investigational
16	ZINC1298	Codeine N-oxide analog	C5	-6.8	332	Investigational
17	ZINC805	Macrolide terpenoid	C5	-6.7	332	Investigational
18	ZINC271	Ethotoin	C3	-6.6	531	Anticonvulsant (approved)
19	ZINC881	Aminoacyl cyclitol antibiotic	C4	-5.8	437	Investigational

** = best pocket per compound.*

Table 2 Binding Pocket Summary for GPR68 CurPocket Analysis.

Pocket	Volume (Å³)	Center (x,y,z)	Preferred by	Best Score	Notes
C5	332	-18, 0, -4	ZINC408, ZINC944, ZINC81, ZINC155, ZINC14, ZINC554, ZINC583, ZINC649, ZINC744, ZINC805, ZINC890, ZINC970, ZINC1298, ZINC1391	-8.3	Most preferred (14/19)
C4	437	13, 5, -20	ZINC515, ZINC881, ZINC1212	-7.2	2nd most preferred
C3	531	4, 4, -14	ZINC10, ZINC271	-7.8	Preferred by approved drugs
C2	835	-24, 5, 16	None (best)	-7	Secondary site only
C1	1739	-9, -7, 24	None (best)	-6.4	Largest; never preferred

**ZINC10 best pocket is C3; C5 listed for completeness.*

ISSN No:-2456-2165 https://doi.org/10.38124/ijisrt/26oct918

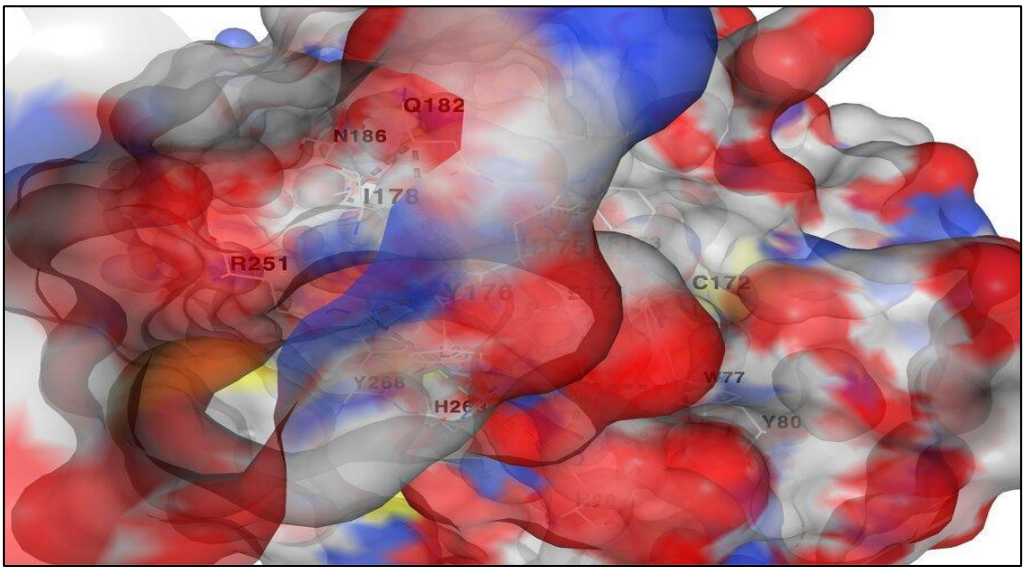


Fig 1 Binding pose of ZINC408 (Tropane-urea hybrid) docked into GPR68 (AF-Q15743-F1-model_v6.pdb). Electrostatic surface coloring: red = electronegative, blue = electropositive, yellow = hydrophobic. Best pocket: C5, Vina score: -8.3 kcal/mol.

Table 3 AutoDock Vina Docking Scores for ZINC408 (Tropane-Urea Hybrid) Across all Five CurPocket Binding Sites on GPR68.

Pocket	Vina (kcal/mol)	Cavity (Å³)	Center (x,y,z)	Dock Box
C5*	-8.3	332	-18, 0, -4	21, 21, 21
C4	-7.7	437	13, 5, -20	21, 21, 21
C2	-7.0	835	-24, 5, 16	21, 21, 21
C3	-7.0	531	4, 4, -14	21, 21, 21
C1	-6.4	1739	-9, -7, 24	21, 21, 21

* = *best-scoring pocket.*

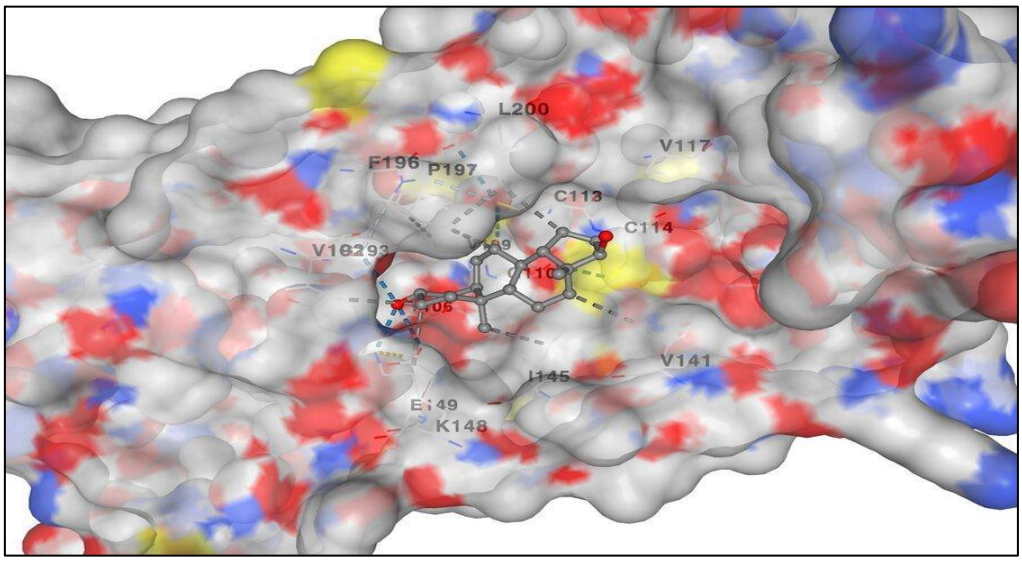


Fig 2 Binding pose of ZINC944 (Steroidal alcohol) docked into GPR68 (AF-Q15743-F1-model_v6.pdb). Electrostatic surface coloring: red = electronegative, blue = electropositive, yellow = hydrophobic. Best pocket: C5, Vina score: -7.9 kcal/mol.

Table 4 AutoDock Vina Docking Scores for ZINC944 (Steroidal Alcohol) Across all Five CurPocket Binding Sites on GPR68.

Pocket	Vina (kcal/mol)	Cavity (Å³)	Center (x,y,z)	Dock Box
C5*	-7.9	332	-18, 0, -4	20, 20, 20
C4	-6.6	437	13, 5, -20	20, 20, 20
C2	-5.8	835	-24, 5, 16	20, 20, 20
C1	-5.5	1739	-9, -7, 24	20, 20, 20
C3	-1.3	531	4, 4, -14	20, 20, 20

* = *best-scoring pocket.*

ISSN No:-2456-2165 https://doi.org/10.38124/ijisrt/26oct918

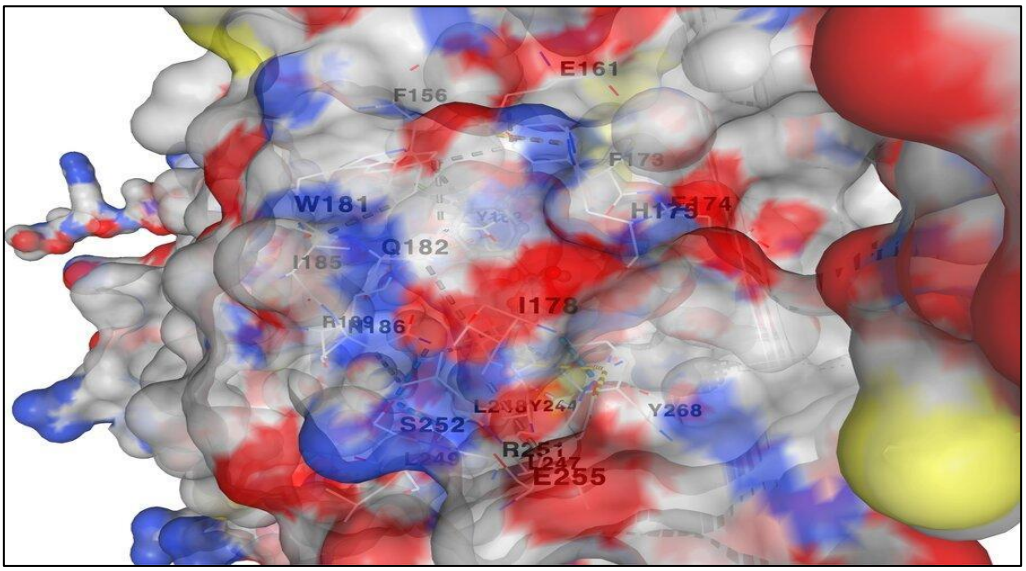


Fig 3 Binding pose of ZINC10 (Acifran) docked into GPR68 (AF-Q15743-F1-model_v6.pdb). Electrostatic surface coloring: red = electronegative, blue = electropositive, yellow = hydrophobic. Best pocket: C3, Vina score: -7.8 kcal/mol.

Table 5 AutoDock Vina Docking Scores for ZINC10 (Acifran) Across all Five CurPocket Binding Sites on GPR68.

Pocket	Vina (kcal/mol)	Cavity (Å³)	Center (x,y,z)	Dock Box
C3*	-7.8	531	4, 4, -14	19, 19, 19
C5	-6.9	332	-18, 0, -4	19, 19, 19
C4	-6.2	437	13, 5, -20	19, 19, 19
C2	-5.4	835	-24, 5, 16	19, 19, 19
C1	-5.3	1739	-9, -7, 24	19, 19, 19

* = *best-scoring pocket.*

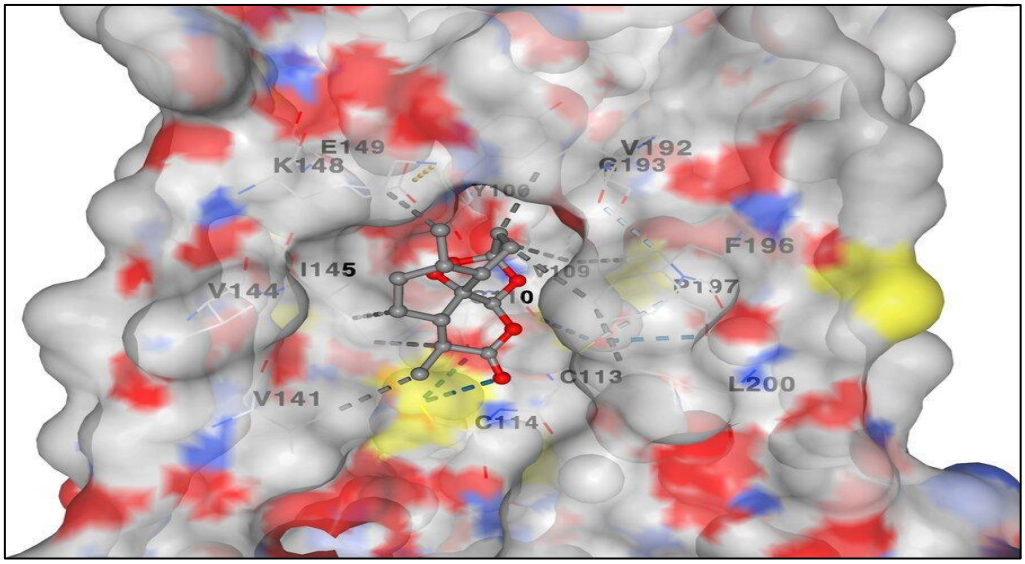


Fig 4 Binding pose of ZINC970 (Terpenoid lactone peroxide) docked into GPR68 (AF-Q15743-F1-model_v6.pdb). Electrostatic surface coloring: red = electronegative, blue = electropositive, yellow = hydrophobic. Best pocket: C5, Vina score: -7.7 kcal/mol.

Table 6 AutoDock Vina Docking Scores for ZINC970 (Terpenoid Lactone Peroxide) Across all Five CurPocket Binding Sites on GPR68.

Pocket	Vina (kcal/mol)	Cavity (Å³)	Center (x,y,z)	Dock Box
C5*	-7.7	332	-18, 0, -4	18, 18, 18
C4	-7.1	437	13, 5, -20	18, 18, 18
C2	-6.3	835	-24, 5, 16	18, 18, 18
C1	-6.1	1739	-9, -7, 24	24, 18, 18
C3	-3.7	531	4, 4, -14	18, 18, 18

* = *best-scoring pocket.*

ISSN No:-2456-2165 https://doi.org/10.38124/ijisrt/26oct918

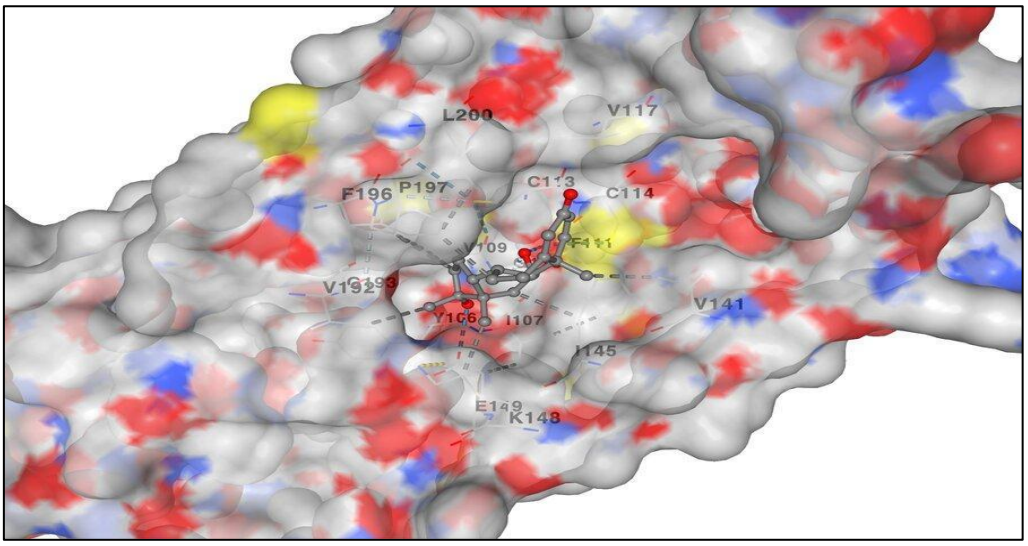


Fig 5 Binding pose of ZINC554 (Steroidal enone) docked into GPR68 (AF-Q15743-F1-model_v6.pdb). Electrostatic surface coloring: red = electronegative, blue = electropositive, yellow = hydrophobic. Best pocket: C5, Vina score: -7.5 kcal/mol.

Table 7 AutoDock Vina Docking Scores for ZINC554 (Steroidal Enone) Across all Five CurPocket Binding Sites on GPR68.

Pocket	Vina (kcal/mol)	Cavity (Å³)	Center (x,y,z)	Dock Box
C5*	-7.5	332	-18, 0, -4	20, 20, 20
C4	-6.5	437	13, 5, -20	20, 20, 20
C2	-6.1	835	-24, 5, 16	20, 20, 20
C1	-4.9	1739	-9, -7, 24	20, 20, 20
C3	-0.2	531	4, 4, -14	20, 20, 20

* = *best-scoring pocket.*

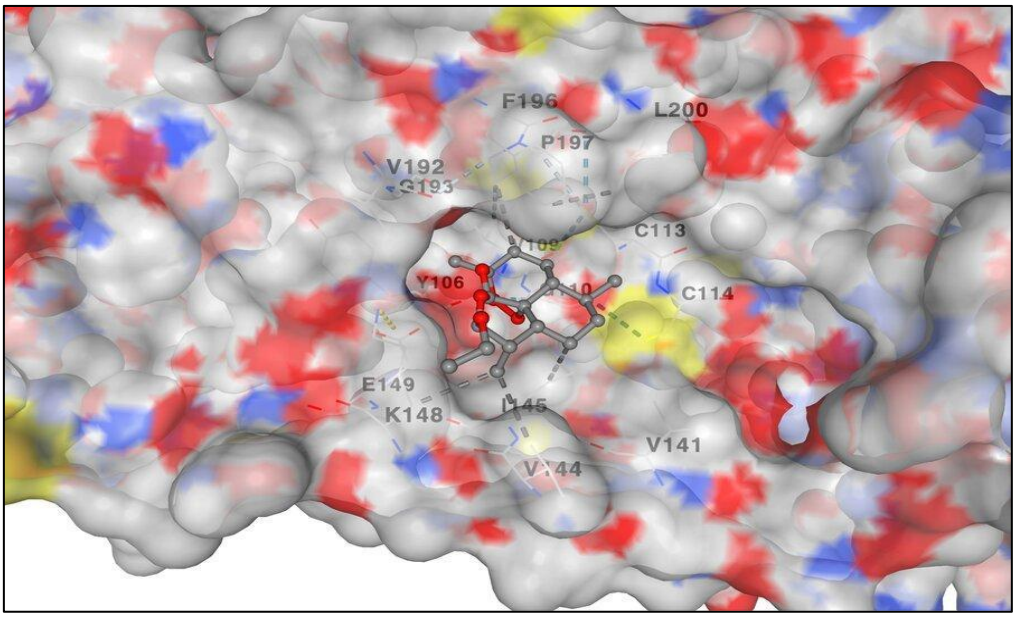


Fig 6 Binding pose of ZINC81 (Terpenoid peroxide) docked into GPR68 (AF-Q15743-F1-model_v6.pdb). Electrostatic surface coloring: red = electronegative, blue = electropositive, yellow = hydrophobic. Best pocket: C5, Vina score: -7.2 kcal/mol.

Table 8 AutoDock Vina Docking Scores for ZINC81 (Terpenoid Peroxide) Across all Five CurPocket Binding Sites on GPR68.

Pocket	Vina (kcal/mol)	Cavity (Å³)	Center (x,y,z)	Dock Box
C5*	-7.2	332	-18, 0, -4	19, 19, 19
C4	-6.6	437	13, 5, -20	19, 19, 19
C1	-5.8	1739	-9, -7, 24	19, 19, 19
C2	-5.5	835	-24, 5, 16	19, 19, 19
C3	-1.9	531	4, 4, -14	19, 19, 19

* = *best-scoring pocket.*

ISSN No:-2456-2165 https://doi.org/10.38124/ijisrt/26oct918

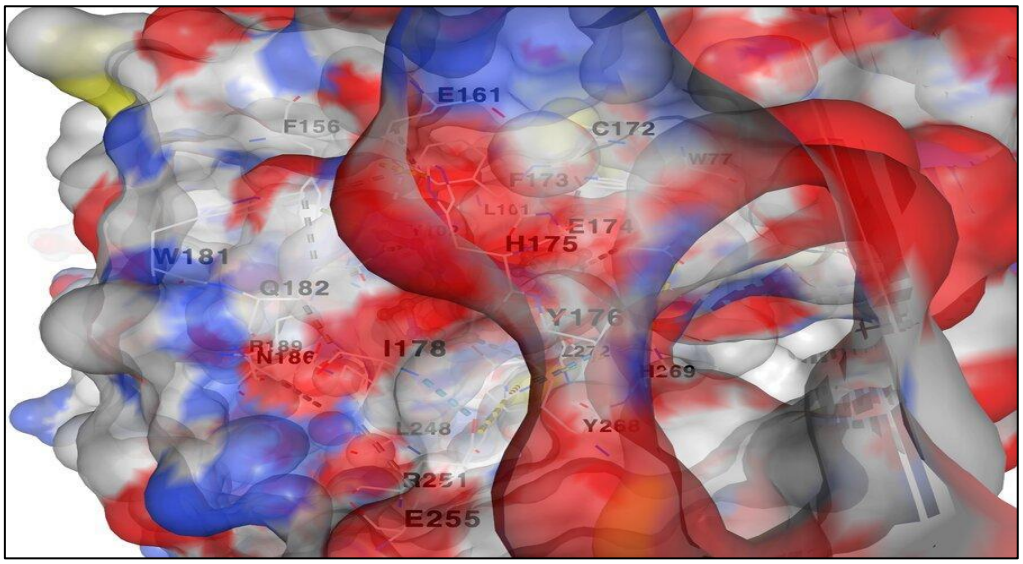


Fig 7 Binding pose of ZINC1212 (Benzoylecgonine methyl ester analog) docked into GPR68 (AF-Q15743-F1-model_v6.pdb). Electrostatic surface coloring: red = electronegative, blue = electropositive, yellow = hydrophobic. Best pocket: C4, Vina score: -7.2 kcal/mol.

Table 9 AutoDock Vina Docking Scores for ZINC1212 (Benzoylecgonine Methyl Ester Analog) Across all Five CurPocket Binding Sites on GPR68.

Pocket	Vina (kcal/mol)	Cavity (Å³)	Center (x,y,z)	Dock Box
C4*	-7.2	437	13, 5, -20	20, 20, 20
C3	-7.1	531	4, 4, -14	20, 20, 20
C5	-6.4	332	-18, 0, -4	20, 20, 20
C2	-5.9	835	-24, 5, 16	20, 20, 20
C1	-5.6	1739	-9, -7, 24	20, 20, 20

** = best-scoring pocket.*

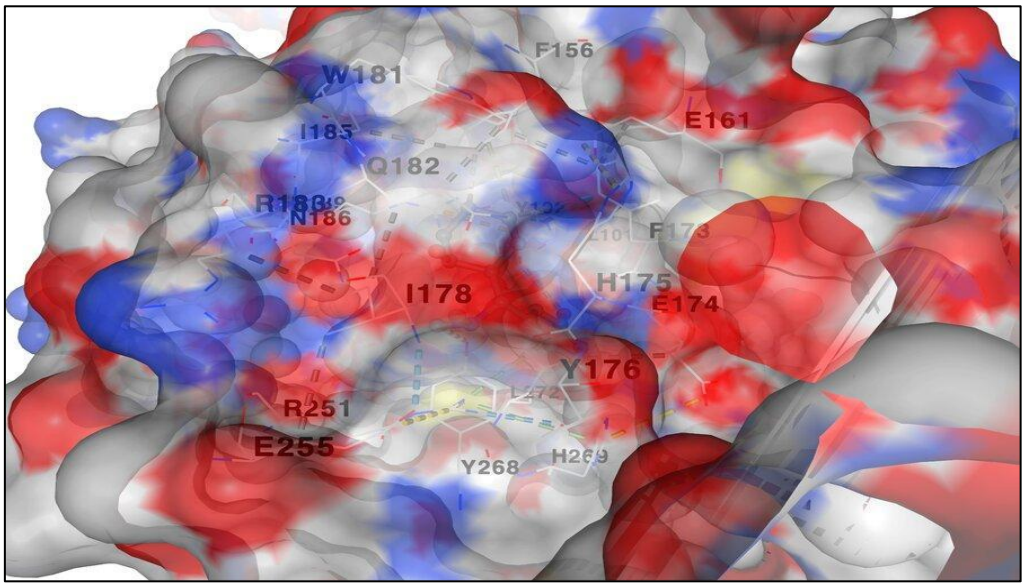


Fig 8 Binding pose of ZINC155 (Phenolic amino alcohol) docked into GPR68 (AF-Q15743-F1-model_v6.pdb). Electrostatic surface coloring: red = electronegative, blue = electropositive, yellow = hydrophobic. Best pocket: C5, Vina score: -7.1 kcal/mol.

Table 10 AutoDock Vina Docking Scores for ZINC155 (Phenolic Amino Alcohol) Across all Five CurPocket Binding Sites on GPR68.

Pocket	Vina (kcal/mol)	Cavity (Å³)	Center (x,y,z)	Dock Box
C5*	-7.1	332	-18, 0, -4	19, 19, 19
C4	-6.5	437	13, 5, -20	19, 19, 19
C1	-5.8	1739	-9, -7, 24	19, 19, 19

ISSN No:-2456-2165 https://doi.org/10.38124/ijisrt/26oct918

C2	-5.6	835	-24, 5, 16	19, 19, 19
C3	-1.8	531	4, 4, -14	19, 19, 19

* = *best-scoring pocket.*

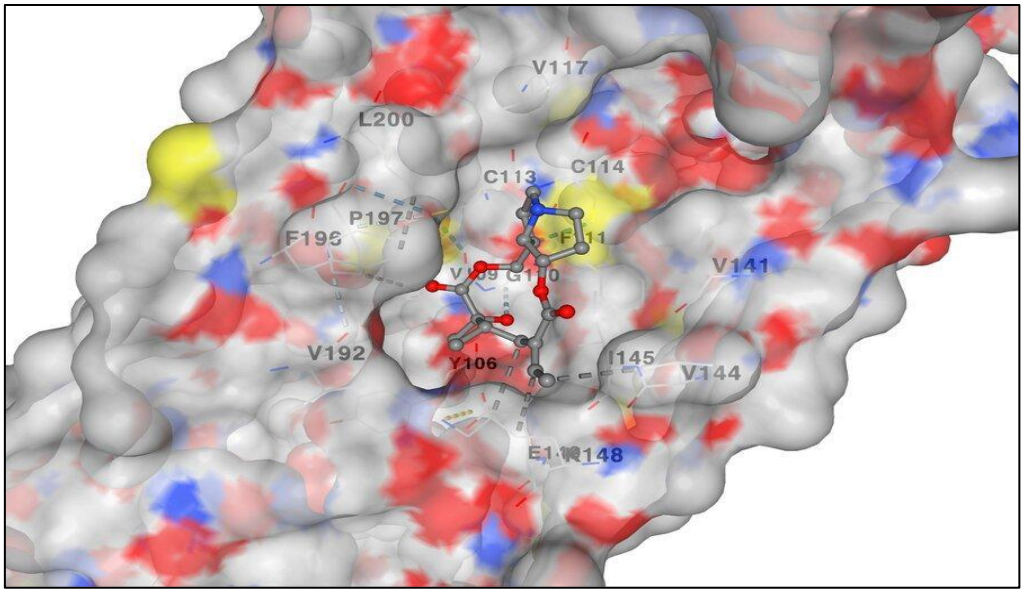


Fig 9 Binding Pose of ZINC649 (Macrocyclic ester alkaloid) docked into GPR68 (AF-Q15743-F1-model_v6.pdb). Electrostatic surface coloring: red = electronegative, blue = electropositive, yellow = hydrophobic. Best pocket: C5, Vina score: -7.1 kcal/mol.

Table 11 AutoDock Vina Docking Scores for ZINC649 (Macrocyclic Ester Alkaloid) Across all Five CurPocket Binding Sites on GPR68.

Pocket	Vina (kcal/mol)	Cavity (Å³)	Center (x,y,z)	Dock Box
C5*	-7.1	332	-18, 0, -4	20, 20, 20
C2	-6.2	835	-24, 5, 16	20, 20, 20
C4	-6.0	437	13, 5, -20	20, 20, 20
C1	-5.0	1739	-9, -7, 24	20, 20, 20
C3	4.7	531	4, 4, -14	20, 20, 20

* = *best-scoring pocket.*

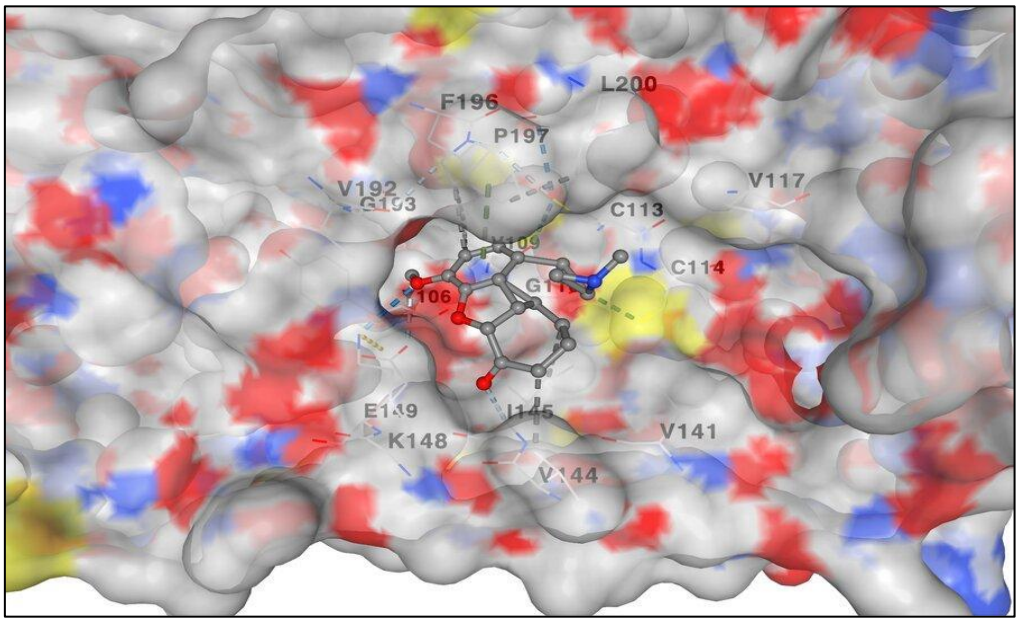


Fig 10 Binding pose of ZINC583 (Isoquinoline alkaloid) docked into GPR68 (AF-Q15743-F1-model_v6.pdb). Electrostatic surface coloring: red = electronegative, blue = electropositive, yellow = hydrophobic. Best pocket: C5, Vina score: -7 kcal/mol.

ISSN No:-2456-2165 https://doi.org/10.38124/ijisrt/26oct918

Table 12 AutoDock Vina Docking Scores for ZINC583 (Isoquinoline Alkaloid) Across all Five CurPocket Binding Sites on GPR68.

Pocket	Vina (kcal/mol)	Cavity (Å³)	Center (x,y,z)	Dock Box
C5*	-7.0	332	-18, 0, -4	19, 19, 19
C4	-6.2	437	13, 5, -20	19, 19, 19
C2	-6.1	835	-24, 5, 16	19, 19, 19
C1	-5.4	1739	-9, -7, 24	19, 19, 19
C3	-3.4	531	4, 4, -14	19, 19, 19

* = *best-scoring pocket.*

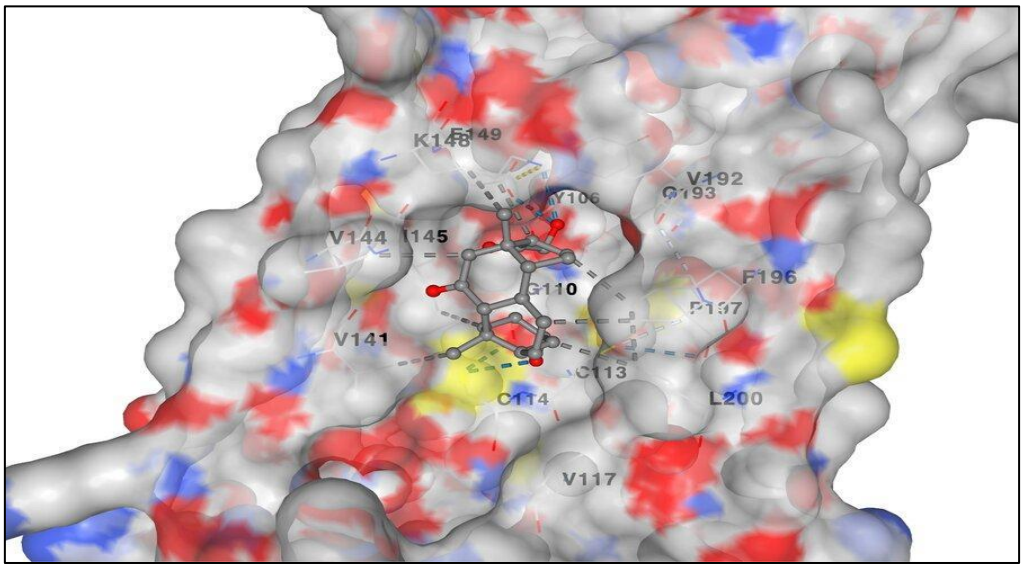


Fig 11 Binding pose of ZINC890 (Steroidal diketone) docked into GPR68 (AF-Q15743-F1-model_v6.pdb). Electrostatic surface coloring: red = electronegative, blue = electropositive, yellow = hydrophobic. Best pocket: C5, Vina score: -7 kcal/mol.

Table 13 AutoDock Vina Docking Scores for ZINC890 (Steroidal Diketone) Across all Five CurPocket Binding Sites on GPR68.

Pocket	Vina (kcal/mol)	Cavity (Å³)	Center (x,y,z)	Dock Box
C5*	-7.0	332	-18, 0, -4	20, 20, 20
C4	-6.0	437	13, 5, -20	20, 20, 20
C2	-5.8	835	-24, 5, 16	20, 20, 20
C1	-4.7	1739	-9, -7, 24	20, 20, 20
C3	-1.2	531	4, 4, -14	20, 20, 20

* = *best-scoring pocket.*

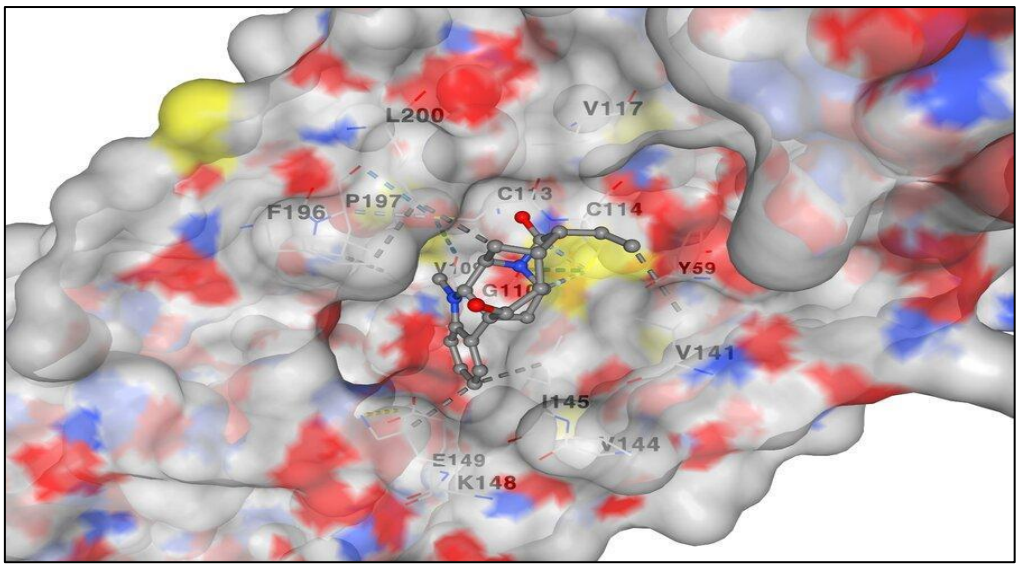


Fig 12 Binding Pose of ZINC14 (Galanthamine-type alkaloid) docked into GPR68 (AF-Q15743-F1-model_v6.pdb). Electrostatic surface coloring: red = electronegative, blue = electropositive, yellow = hydrophobic. Best pocket: C5, Vina score: -6.9 kcal/mol.

ISSN No:-2456-2165 https://doi.org/10.38124/ijisrt/26oct918

Table 14 AutoDock Vina Docking Scores for ZINC14 (Galanthamine-Type Alkaloid) Across all Five CurPocket Binding Sites on GPR68.

Pocket	Vina (kcal/mol)	Cavity (Å³)	Center (x,y,z)	Dock Box
C5*	-6.9	332	-18, 0, -4	20, 20, 20
C4	-6.7	437	13, 5, -20	20, 20, 20
C2	-6.2	835	-24, 5, 16	20, 20, 20
C1	-5.8	1739	-9, -7, 24	20, 20, 20
C3	2.4	531	4, 4, -14	20, 20, 20

* = *best-scoring pocket.*

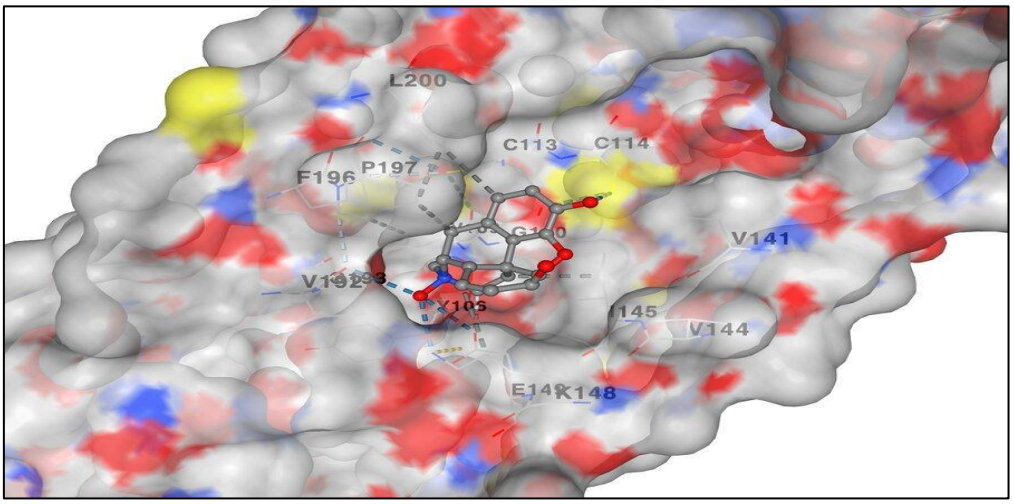


Fig 13 Binding pose of ZINC515 (Morphine-like N-oxide alkaloid) docked into GPR68 (AF-Q15743-F1-model_v6.pdb). Electrostatic surface coloring: red = electronegative, blue = electropositive, yellow = hydrophobic. Best pocket: C4, Vina score: -6.9 kcal/mol.

Table 15 AutoDock Vina Docking Scores for ZINC515 (Morphine-Like N-Oxide Alkaloid) Across all Five CurPocket Binding Sites on GPR68.

Pocket	Vina (kcal/mol)	Cavity (Å³)	Center (x,y,z)	Dock Box
C4*	-6.9	437	13, 5, -20	19, 19, 19
C5	-6.9	332	-18, 0, -4	19, 19, 19
C2	-6.2	835	-24, 5, 16	19, 19, 19
C1	-5.0	1739	-9, -7, 24	19, 19, 19
C3	0.0	531	4, 4, -14	19, 19, 19

* = *best-scoring pocket.*

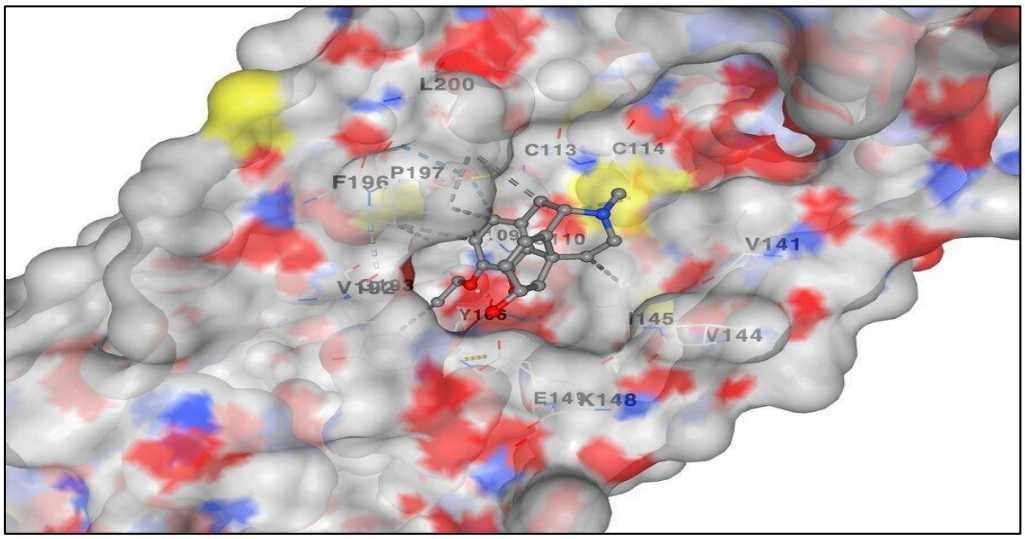


Fig 14 Binding pose of ZINC1391 (Ethoxy isoquinoline alkaloid) docked into GPR68 (AF-Q15743-F1-model_v6.pdb). Electrostatic surface coloring: red = electronegative, blue = electropositive, yellow = hydrophobic. Best pocket: C5, Vina score: -6.9 kcal/mol.

ISSN No:-2456-2165 https://doi.org/10.38124/ijisrt/26oct918

Table 16 AutoDock Vina docking scores for ZINC1391 (Ethoxy isoquinoline alkaloid) across all five CurPocket binding sites on GPR68.

Pocket	Vina (kcal/mol)	Cavity (Å³)	Center (x,y,z)	Dock Box
C5*	-6.9	332	-18, 0, -4	19, 19, 19
C4	-6.4	437	13, 5, -20	19, 19, 19
C2	-6.3	835	-24, 5, 16	19, 19, 19
C1	-5.3	1739	-9, -7, 24	19, 19, 19
C3	0.2	531	4, 4, -14	19, 19, 19

* = *best-scoring pocket.*

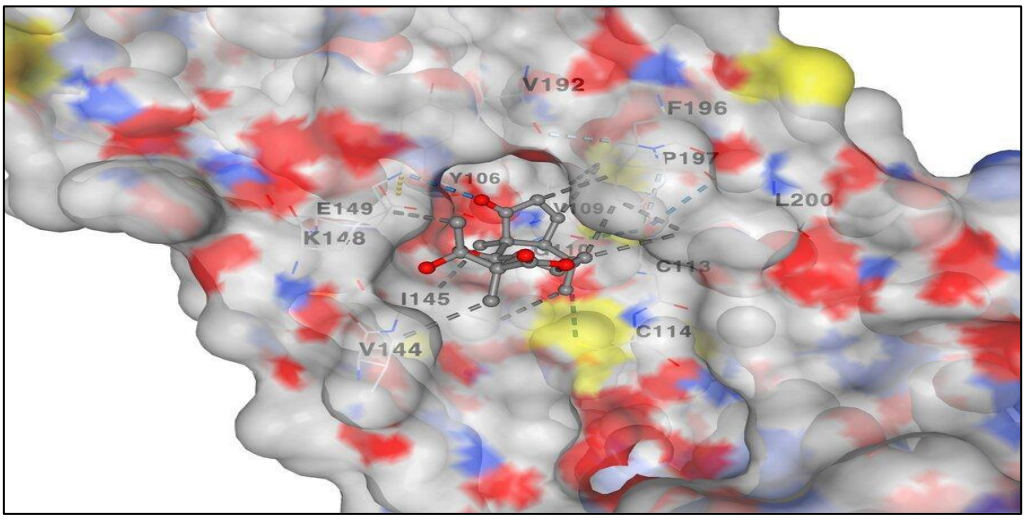


Fig 15 Binding pose of ZINC744 (Tricyclic terpenoid lactone) docked into GPR68 (AF-Q15743-F1-model_v6.pdb). Electrostatic surface coloring: red = electronegative, blue = electropositive, yellow = hydrophobic. Best pocket: C5, Vina score: -6.8 kcal/mol.

Table 17 AutoDock Vina docking scores for ZINC744 (Tricyclic terpenoid lactone) across all five CurPocket binding sites on GPR68.

Pocket	Vina (kcal/mol)	Cavity (Å³)	Center (x,y,z)	Dock Box
C5*	-6.8	332	-18, 0, -4	18, 18, 18
C2	-6.3	835	-24, 5, 16	18, 18, 18
C4	-6.0	437	13, 5, -20	18, 18, 18
C1	-5.5	1739	-9, -7, 24	24, 18, 18
C3	-2.4	531	4, 4, -14	18, 18, 18

* = *best-scoring pocket.*

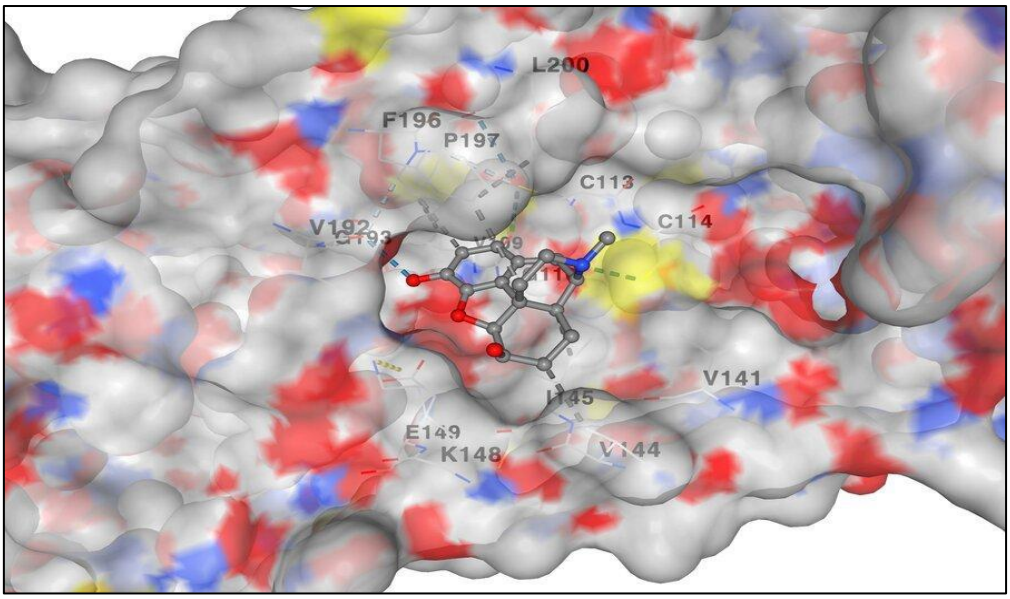


Fig 16 Binding pose of ZINC1298 (Codeine N-oxide analog) docked into GPR68 (AF-Q15743-F1-model_v6.pdb). Electrostatic surface coloring: red = electronegative, blue = electropositive, yellow = hydrophobic. Best pocket: C5, Vina score: -6.8 kcal/mol.

ISSN No:-2456-2165 https://doi.org/10.38124/ijisrt/26oct918

Table 18 AutoDock Vina docking scores for ZINC1298 (Codeine N-oxide analog) across all five CurPocket binding sites on GPR68.

Pocket	Vina (kcal/mol)	Cavity (Å³)	Center (x,y,z)	Dock Box
C5*	-6.8	332	-18, 0, -4	18, 18, 18
C2	-6.5	835	-24, 5, 16	18, 18, 18
C4	-6.5	437	13, 5, -20	18, 18, 18
C1	-6.4	1739	-9, -7, 24	24, 18, 18
C3	-1.1	531	4, 4, -14	18, 18, 18

* = *best-scoring pocket.*

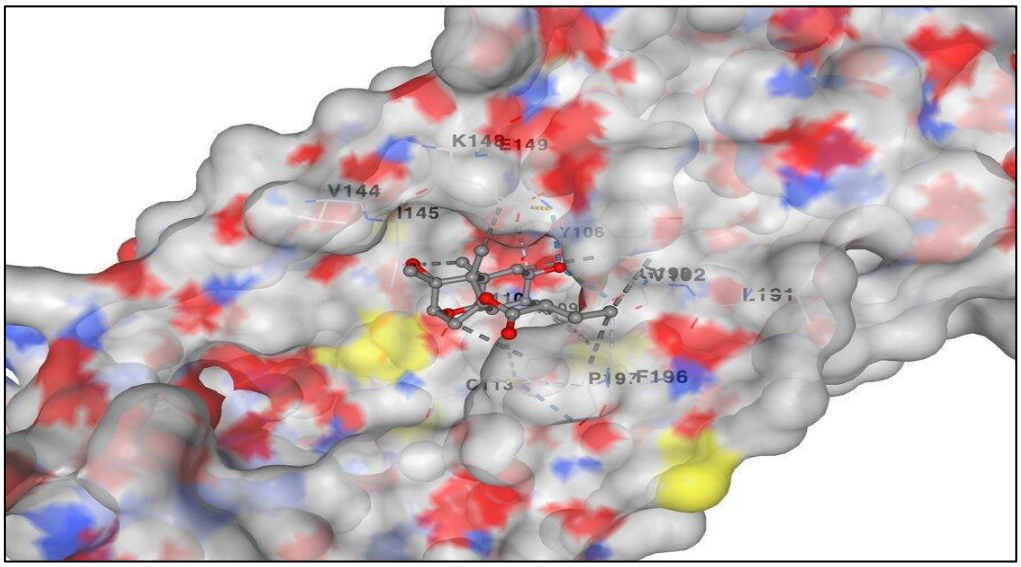


Fig 17 Binding pose of ZINC805 (Macrolide terpenoid) docked into GPR68 (AF-Q15743-F1-model_v6.pdb). Electrostatic surface coloring: red = electronegative, blue = electropositive, yellow = hydrophobic. Best pocket: C5, Vina score: -6.7 kcal/mol.

Table 19 AutoDock Vina docking scores for ZINC805 (Macrolide terpenoid) across all five CurPocket binding sites on GPR68.

Pocket	Vina (kcal/mol)	Cavity (Å³)	Center (x,y,z)	Dock Box
C5*	-6.7	332	-18, 0, -4	21, 21, 21
C4	-6.4	437	13, 5, -20	21, 21, 21
C2	-5.9	835	-24, 5, 16	21, 21, 21
C1	-5.7	1739	-9, -7, 24	21, 21, 21
C3	-1.7	531	4, 4, -14	21, 21, 21

* = *best-scoring pocket.*

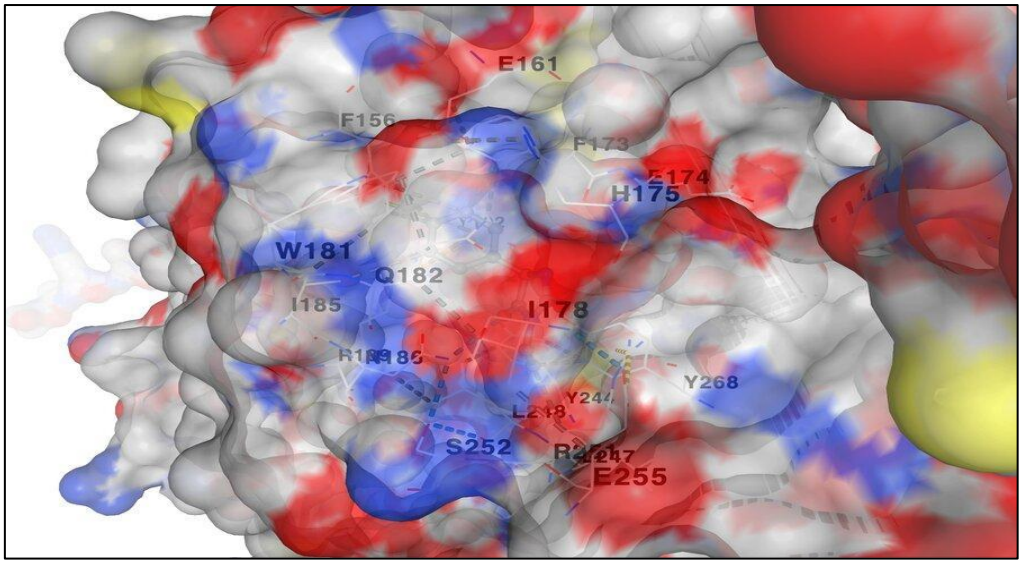


Fig 18 Binding pose of ZINC271 (Ethotoin) docked into GPR68 (AF-Q15743-F1-model_v6.pdb). Electrostatic surface coloring: red = electronegative, blue = electropositive, yellow = hydrophobic. Best pocket: C3, Vina score: -6.6 kcal/mol.

ISSN No:-2456-2165 https://doi.org/10.38124/ijisrt/26oct918

Table 20 AutoDock Vina docking scores for ZINC271 (Ethotoin) across all five CurPocket binding sites on GPR68.

Pocket	Vina (kcal/mol)	Cavity (Å³)	Center (x,y,z)	Dock Box
C3*	-6.6	531	4, 4, -14	18, 18, 18
C4	-6.2	437	13, 5, -20	18, 18, 18
C1	-5.7	1739	-9, -7, 24	24, 18, 18
C5	-5.5	332	-18, 0, -4	18, 18, 18
C2	-5.3	835	-24, 5, 16	18, 18, 18

* = *best-scoring pocket.*

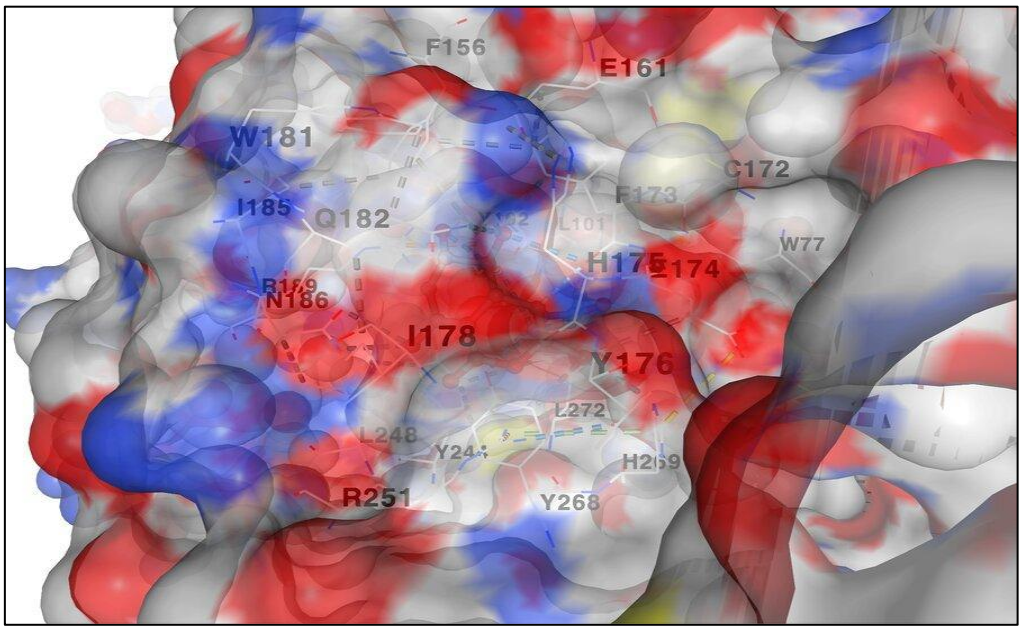


Fig 19 Binding pose of ZINC881 (Aminoacyl cyclitol antibiotic) docked into GPR68 (AF-Q15743-F1-model_v6.pdb). Electrostatic surface coloring: red = electronegative, blue = electropositive, yellow = hydrophobic. Best pocket: C4, Vina score: -5.8 kcal/mol.

Table 21 AutoDock Vina docking scores for ZINC881 (Aminoacyl cyclitol antibiotic) across all five CurPocket binding sites on GPR68.

Pocket	Vina (kcal/mol)	Cavity (Å³)	Center (x,y,z)	Dock Box
C4*	-5.8	437	13, 5, -20	19, 19, 19
C5	-5.8	332	-18, 0, -4	19, 19, 19
C3	-5.7	531	4, 4, -14	19, 19, 19
C2	-5.2	835	-24, 5, 16	19, 19, 19
C1	-4.3	1739	-9, -7, 24	19, 19, 19

* = *best-scoring pocket.*